Fetal Diagnosis and Therapy

Research Article

Fetal Diagn Ther 2020;47:902–911
DOI: 10.1159/000509244

Received: December 30, 2019
Accepted: June 6, 2020
Published online: September 2, 2020

Initial Mechanistic Screening of Transamniotic Stem Cell Therapy in the Rodent Model of Spina Bifida: Host Bone Marrow and Paracrine Activity

Stefanie P. Lazow Sarah A. Tracy Alexander V. Chalphin Ina Kycia
David Zurakowski Dario O. Fauza

Department of Surgery, Boston Children's Hospital and Harvard Medical School, Boston, MA, USA

Keywords
Spina bifida · Myelomeningocele · Transamniotic stem cell therapy · Amniotic mesenchymal stem cell · Amniotic stem cell · Fetal stem cell

Abstract
Purpose: Transamniotic stem cell therapy (TRASCET) with mesenchymal stem cells (MSCs) can induce spina bifida coverage with neoskin. We initiated a mechanistic analysis of this host response. ***Methods:*** Pregnant dams ($n = 28$) exposed to retinoic acid to induce fetal spina bifida were divided into an untreated group and 2 groups receiving intra-amniotic injections on gestational day 17 (E17; term = E21–22) of either amniotic fluid-derived MSCs (afMSCs; $n = 105$) or saline ($n = 107$). Gene expressions of multiple paracrine and cell clonality markers were quantified at term by RT-qPCR at the defect and fetal bone marrow. Defects were examined histologically for neoskin coverage. Comparisons were by Mann-Whitney U tests and logistic regression. ***Results:*** Defect coverage was associated with significant downregulation of both epidermal growth factor (*Egf*; $p = 0.031$) and fibroblast growth factor-2 (*Fgf-2*; $p = 0.042$) expressions at the defect and with significant downregulation of transforming growth factor-beta-1 (*Tgfb*-1; $p = 0.021$) and *CD45* ($p = 0.028$) expressions at the fetal bone marrow. ***Conclusions:*** Coverage of experimental spina bifida is associated with local and bone marrow negative feedback of select paracrine factors, as well as increased relative mesenchymal stem cell activity in the bone marrow. Further analyses informed by these findings may lead to strategies of nonsurgical induction of prenatal coverage of spina bifida.

Introduction

Transamniotic stem cell therapy (TRASCET) has emerged experimentally as a novel alternative for the prenatal management of diverse congenital anomalies [1]. Such broad applicability is thought to be related to the fact that the donor cell most commonly used for TRASCET, the amniotic fluid-derived mesenchymal stem cell (afMSC), has been shown to play a central role in the

Presented as oral presentation at the 38th Annual Meeting of the International Fetal Medicine and Surgery Society, October 22–26, 2019, Sils, Switzerland.

Dario O. Fauza,
Department of Surgery, Boston Children's Hospital
300 Longwood Avenue, Fegan 3
Boston 02115 (USA)
dario.fauza@childrens.harvard.edu

fetus' ability to repair tissue damage [2]. In spina bifida, TRASCET performed with either afMSCs or placental mesenchymal stem cells (pMSCs) has been shown to enhance the formation of a host-derived neoskin either partially or completely covering the defect in both rodent and leporine models of the disease [3–6]. Interestingly, however, donor MSCs have not been found within the neoskin coverage. Instead, they have been noted to home robustly to the fetal bone marrow via a hematogenous route, particularly in the setting of this congenital anomaly [3, 7, 8]. This has led us to hypothesize that the effects of TRASCET in spina bifida are centered on host bone marrow activity via a substantial magnification of naturally occurring processes. In this study, we start to test this hypothesis by investigating the expression of select paracrine factors in both the bone marrow and the defect itself, as well as by profiling specific markers of bone marrow cell clonality.

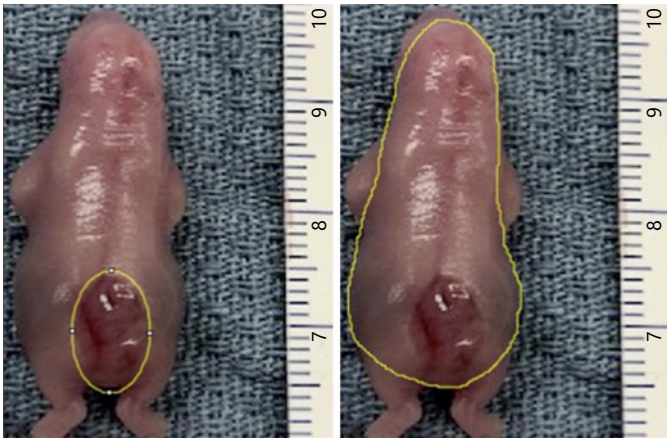

Color version available online

Fig. 1. The left image depicts the measurement of the fetal spina bifida defect area by fitting an ellipse to the defect. The right image depicts the measurement of the fetal total dorsum area by freehand tracing (right) using ImageJ software.

Materials and Methods

This study was approved by the Boston Children's Hospital Institutional Animal Care and Use Committee under protocol # 18-07-3757R.

Donor afMSC Processing

Donor afMSCs consisted of banked unlabeled cells previously derived from normal syngeneic Lewis rat dams after amniotic fluid procurement under direct vision through an open laparotomy performed on gestational day 21 (E21; term = 21–22 days), followed by isolation and expansion based on methods as previously described [9, 10]. Fluorescence-activated cell sorting (FACS) analysis with the Vantage SE cell sorter (Becton Dickinson Biosciences, East Rutherford, NJ, USA) was used to confirm the mesenchymal progenitor identity of the donor afMSCs with primary conjugated mouse monoclonal antibodies previously validated for use in rats, namely, for CD29 (Becton Dickinson Biosciences), CD44 (R&D Systems, Minneapolis, MN, USA), and CD90 (Becton Dickinson Biosciences) with negativity for CD45 (Invitrogen, Grand Island, NY, USA). A purified CD73 (Becton Dickinson Biosciences) conjugated with an anti-mouse IgG1 against purified CD73 (Biolegend, San Diego, CA, USA) was also used. Nonspecific cell staining was excluded using mouse isotype immunoglobulin controls.

Fetal Spina Bifida Creation and Intra-Amniotic Injections

Twenty-eight time-dated pregnant Sprague Dawley dams (Charles River Laboratories, Inc., Wilmington, MA, USA) were fed a normal diet ad libitum and housed individually under standard dark/light cycling conditions. All animals received retinoic acid for the induction of fetal neural tube defects on gestational day 10 (E10), as previously described [11]. In brief, after exposure to isoflurane (Abbott Laboratories, North Chicago, IL, USA), chamber inhaled at 2–4% in 100% oxygen, the dams received 60 mg/kg of all-trans retinoic acid (Sigma-Aldrich, St. Louis, MO, USA) dissolved in olive oil at 10 mg/mL at room temperature via orogastric gavage performed between 6:00 p.m. and 8:00 p.m. Animals were then divided into 3 groups. One group (untreated) underwent no further manipulations (their number of fetuses could only be determined at euthanasia). The other 2 groups received volume-matched (50 μL) intra-amniotic injections of either saline ($n = 107$) or a concentrated suspension of 2×10^6 cells/mL afMSCs ($n = 105$) at E17. Injected donor cells were at passages 9–15.

For all intra-amniotic injections, general anesthesia was induced and maintained with isoflurane (Patterson Veterinary, Greeley, CO, USA), chamber inhaled at 1.5–3% in 100% oxygen. The bicornuate uterus was eviscerated via a midline laparotomy to allow for controlled injection into each amniotic cavity of a given dam, under direct vision. A 33-G noncoring needle (Hamilton Company, Reno, NV, USA) on a 100 μL syringe (Hamilton Company) was introduced into the cavity by the ventral aspect of the fetus. Care was taken to avoid injection into the fetus, placenta, or umbilical cord. After the procedure, the uterus was returned to the abdomen and the laparotomy was closed in 2 layers with 3-0 Vicryl (Ethicon, Somerville, NJ, USA) and 5-0 Monocryl (Ethicon) simple running sutures. Animals were allowed to recover with no additional manipulations other than powdered Flagyl (Unichem Pharmaceuticals, Hasbrouck Heights, NJ, USA) on the wound and analgesia with subcutaneous injections of sustained release buprenorphine (Zoopharm, Windsor, CO, USA).

Defect Procurement and Histological Analysis

Dams were euthanized with chamber-inhaled carbon dioxide at E21 just before term. A midline incision was made, and the uterus was eviscerated. The myometrium and gestational membranes were cut sharply, and the umbilical cord was transected. Each fetus was inspected grossly for the presence of a neural tube defect and any additional malformations. Fetuses with combined spina bifida and other defects, such as exencephaly and/or gastroschisis, were excluded. Fetuses with isolated spina bifida were then uniformly photographed in the prone position next to a ruler for scale. ImageJ software (U.S. National Institutes of Health, Bethesda, MD, USA) was used to measure the area of the spina

Table 1. Primer sequences for RT-qPCR

Gene	Forward primer	Reverse primer
GAPDH	5′-CTGAACGGGAAGCTCACTGG-3′	5′-ATACTTGGCAGGTTTCTCCAGG-3′
β-actin	5′-AGCAAGCAGGAGTACGATGAG-3′	5′-GAAAGGGTGTAAAACGCAGCTC-3′
Fgf-2/b-Fgf	5′-CGACCCACACGTCAAACTACA-3′	5′-CAGCCGTCCATCTTCCTTCAT-3′
Vegf-a	5′-TTGTCCAAGATCCGCAGACG-3′	5′-GCTTGTCACATCTGCAAGTACG-3′
Egf	5′-TGGGATCTACTGTCTCGACGTT-3′	5′-TGCAGTTGTAGCCTCCCTCC-3′
Tgfb-3	5′-GCAAGAATCTGCCCACGAGA-3′	5′-CCCAAGTTGGACTCTCTCCG-3′
Tgfb-1	5′-ATACCAACTACTGCTTCAGCTCC-3′	5′-GATCCACTTCCAACCCAGGTC-3′
Cox-2	5′-CAGATTGCTGGCCGGGTTG-3′	5′-TCATCTCTCTGCTCTGGTCAATG-3′
Ptprc/CD45	5′-GTATTGCTCAAAGCTGCCCAC-3′	5′-CTCCTGGAAAGTGCAGAAACAG-3′
Snai1	5′-CGCGCTCCTTCCTGGTC-3′	5′-GCTGGAAGGTGAACTCCACA-3′
Vcam-1/CD106	5′-GCACACTTCCACAAGTACAGG-3′	5′-TGAACTGATTATCCAAGGCTCTTC-3′
Mcam/CD146	5′-CGCAAGAGAATGCAATGCTG-3′	5′-GTTCCATTCAGTTGCCGAGC-3′
Msx2	5′-CGTCAAGCCCTTCGAGACC-3′	5′-GGCTCATGTGTCTGGGCG-3′
Thy1/CD90	5′-GAGGGCGACTACATGTGTGA-3′	5′-CACTTGACCAGCTTGTCTCTGA-3′
Endoglin/CD105	5′-TATTCTCACACACGTGCCCC-3′	5′-CCGATCCTGTGGTTGGTACT-3′

Egf, epidermal growth factor; *Fgf-2*, fibroblast growth factor-2; *Tgfb-3*, transforming growth factor-beta-3; *Tgfb-1*, transforming growth factor-beta-1; *Vegf-a*, vascular endothelial growth factor-a.

bifida defect and the total dorsum area; these measurements were then used to create a ratio of defect area to total dorsum area per fetus (Fig. 1).

The spina bifida defect was then dissected and separated from the fetus with a rim of surrounding normal skin and underlying tissue. The defect was then split in half transversely to allow for correlated histological and RT-qPCR analysis of each hemidefect. The half of the defect allocated for RT-qPCR underwent further dissection with removal of the underlying tissue to isolate the most superficial, exposed layer of the defect and any eventual overlying skin coverage; the rim of surrounding normal skin tissue was left intact. The other half of the defect allocated for histology was then immediately immersed in 10% neutral buffered formalin at room temperature for at least 72 h. Histology was performed on fixed paraffin-embedded specimens stained with hematoxylin-eosin (H&E). The presence of defect coverage was determined by 2 blinded observers only if confirmed by the mutual identification of a primitive neoskin, characteristically hypoplastic and with a paucity or absence of adnexa, either partially or completely overlying the defect. All histological examinations were performed with an EVOS® XL Core Imaging System microscope fitted with an onboard computer and integrated imaging software (Life Technologies, Carlsbad, CA, USA).

Bone Marrow Procurement

Fetal bone marrow was procured from both femurs and tibias. In rare cases of insufficient bone marrow from the lower extremities, the marrow was procured from both humerus bones instead or additionally. In either procedure, bones were dissected from surrounding soft tissue and transected proximally and distally to expose the medullary cavity. Specimens were then placed within 0.5 mL Eppendorf tubes punctured with an 18-G needle, which were then placed inside a 1.5 mL Eppendorf tube; both were centrifuged at 15 RCF for 1 min to isolate the bone marrow.

Reverse Transcription Quantitative Polymerase Chain Reaction

RT-qPCR was performed to quantify relative mRNA expression of select paracrine factors at both the defect site and the bone marrow, as well as of markers of MSC clonality within the bone marrow. Total mRNA extraction was performed using TRIzol reagent (Thermo Fisher Scientific, Waltham, MA, USA). cDNA and corresponding negative controls were then synthesized using SuperScript IV First-Strand Synthesis System (Invitrogen). cDNA was subsequently added to appropriate primer sets and Precision MasterMix premixed with SYBR green (Qiagen, Germantown, MD, USA). Primer sequences are listed in Table 1. qPCR was then performed using the CFX96 Touch real-time PCR detection system (Bio-Rad Laboratories, Hercules, CA, USA). Relative mRNA fold expression was calculated using the delta-delta Ct method controlled by defect tissue from the untreated group for defect analysis and by bone marrow from normal fetuses ($n = 32$, from 3 healthy dams) for bone marrow analysis. *GAPDH* was the housekeeping gene for defect analysis, and *β-actin* was the housekeeping gene for bone marrow analysis. A subset of bone marrow samples had to be excluded due to poor mRNA quality.

Statistical Analysis

Each statistical analysis was performed within the subset of fetuses with relevant data available for that analysis. Defect area to total dorsum area ratio was compared between treatment groups using quantile regression while controlling for maternal identity, using conservative Bonferroni-adjusted criteria for multiple treatment group comparisons ($p < 0.017$). The Mann-Whitney U test was used to compare mRNA expression between fetuses with covered and uncovered defects ($p < 0.05$). Given limitations from low power specific to the bone marrow analysis due to the requisite exclusion of samples for poor RNA quality, ROC curves were created for the expression of MSC clonality markers; the Youden index was then utilized to determine the

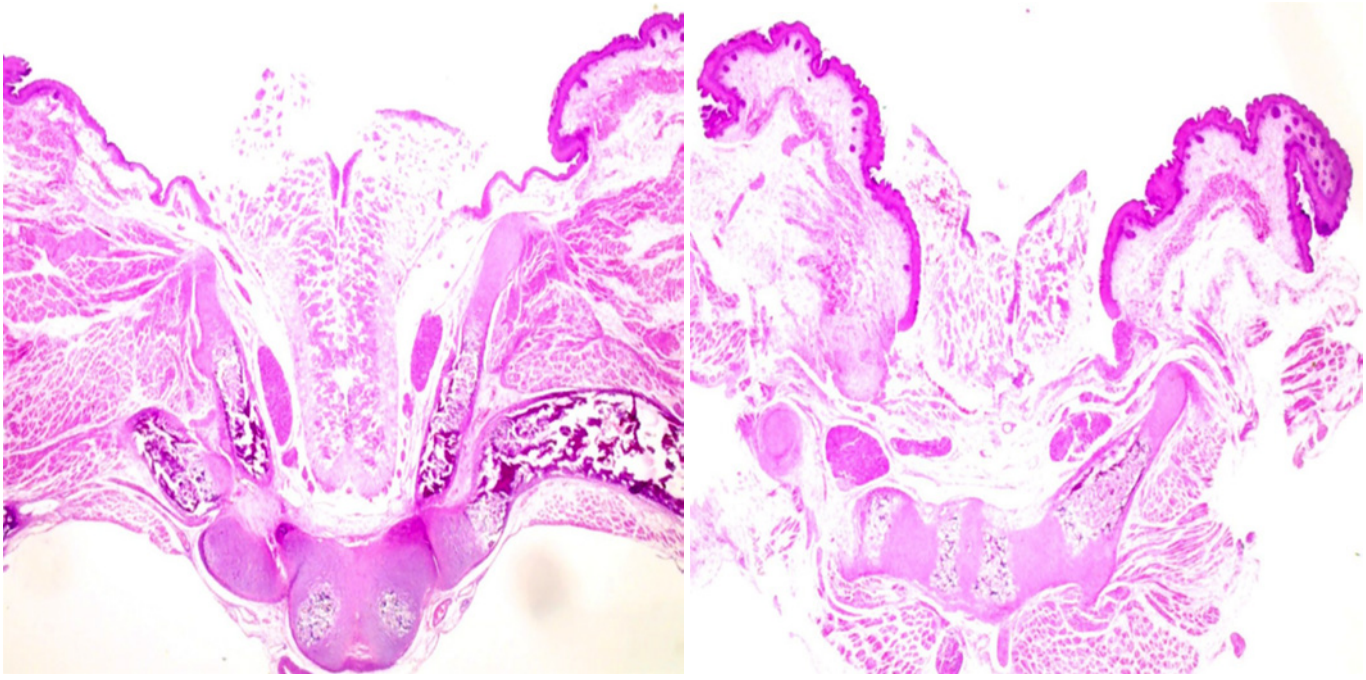

Color version available online

Fig. 2. Representative spina bifida defect with histological partial coverage with a thin layer of rudimentary neoskin (left) and a spina bifida defect lacking neoskin coverage (right). The typical widely open vertebra arches and variably deformed spinal cord are also visible in both images. H&E. ×20.

best threshold to optimize coverage prediction. Logistic regression was then performed to compare fetuses with covered and uncovered defects by this binary fold difference threshold with output reported as the likelihood ratio test (LRT) p value with associated odds ratio.

A Mann-Whitney U test was also used to compare mRNA expression between treatment groups, using conservative Bonferroni-adjusted criteria for multiple treatment group comparisons (defect analysis: $p < 0.017$; bone marrow analysis: $p < 0.0083$). Quantile regression was also used to compare defect site paracrine factor expression between treatment groups while controlling for the defect area to total dorsum area ratio, with a Bonferroni-adjusted criteria for multiple comparisons ($p < 0.017$). Lastly, nonparametric Spearman's correlation was performed to evaluate the relationship between defect and bone marrow paracrine factor expression. Statistical analysis was performed using SPSS version 24.0 (IBM Corporation, Armonk, NY, USA).

Results

Survival

There were 102 survivors with an isolated spina bifida including 36/105 (34.3%) fetuses from the afMSC-injected group, 34/107 (31.8%) fetuses from the saline-injected group, and 32 fetuses from the untreated group. There was no significant difference in survival with an isolated spina bifida between the afMSC-injected and saline-injected groups ($p = 0.698$). The overall maternal mortality was 10.7% (3/28): one death was secondary to oral gavage complications, one was related to anesthesia, and one dam underwent early euthanasia due to preterm labor likely secondary to chorioamnionitis.

Defect Analysis

There were significant differences between treatment groups in the ratio of the spina bifida defect to total fetal dorsum areas, which could be evaluated in 95 fetuses. The afMSC-injected group demonstrated significantly larger defect area to total dorsum area ratio (median: 0.09, IQR: 0.06–0.16) compared with the saline-injected group (median: 0.06, IQR: 0.04–0.09), but not the untreated group (median: 0.09, IQR: 0.07–0.13) on quantile regression analysis controlling for maternal identity ($p < 0.001$ and $p = 0.028$, respectively).

There were 98 hemidefects procured for histological analysis. In 40 of them (40.8%), the quality of the histological preparation prevented a proper screening for the presence of coverage (Fig. 2). Among the histological preparations suitable for analysis, 11/20 (55%) of the

Table 2. Paracrine factor and MSC clonality marker expression in fetuses with covered and uncovered defects[a]

	Covered defects: median fold difference (IQR)	Uncovered defects: median fold difference (IQR)	*p* value*
Paracrine factors: defect			
Fgf-2	0.70 (0.33–1.14)	1.06 (0.62–2.13)	**0.042**
Vegf-a	0.88 (0.47–1.55)	1.08 (0.77–1.51)	0.326
Tgfb-3	0.98 (0.39–1.23)	0.98 (0.79–1.31)	0.490
Tgfb-1	0.86 (0.60–1.07)	0.93 (0.65–1.75)	0.393
Egf	0.80 (0.51–1.11)	1.08 (0.84–1.84)	**0.031**
Cox-2	0.99 (0.32–1.22)	1.29 (0.70–1.94)	0.122
Paracrine factors: bone marrow			
Fgf-2	2.07 (1.77–2.85)	1.67 (0.85–2.35)	0.169
Vegf-a	1.06 (0.92–1.65)	1.28 (0.97–1.64)	0.373
Tgfb-3	1.76 (1.45–2.70)	1.94 (1.50–2.81)	0.793
Tgfb-1	1.14 (0.94–1.42)	1.49 (1.16–1.88)	0.065
Bone marrow MSC clonality markers			
Ptprc/CD45	1.06 (0.86–1.60)	1.53 (1.19–2.07)	0.065
Snai1	1.20 (1.05–1.66)	1.39 (1.10–1.84)	0.387
Vcam-1/CD106	1.64 (1.44–2.88)	1.93 (1.35–2.29)	0.774
Mcam/CD146	1.26 (1.02–1.77)	1.45 (0.87–2.60)	0.415
Msx2	3.64 (1.64–6.33)	2.42 (1.57–3.90)	0.252
Thy1/CD90	1.15 (1.01–1.99)	1.57 (1.01–2.14)	0.680
Endoglin/CD105	1.89 (1.37–3.49)	1.98 (1.51–3.16)	0.832

MSC, mesenchymal stem cell; *Vegf-a*, vascular endothelial growth factor-a; *Egf*, epidermal growth factor; *Fgf-2*, fibroblast growth factor-2; *Tgfb-1*, transforming growth factor-beta-1; *Tgfb-3*, transforming growth factor-beta-3. [a] For defect RT-qPCR analysis: $n = 14$ covered defects and $n = 44$ uncovered defects. For bone marrow RT-qPCR analysis: $n = 10$ covered defects and $n = 38$ uncovered defects. * Statistical significance based on the Mann-Whitney U test ($p < 0.05$).

afMSC-injected fetuses showed partial coverage compared with 3/24 (12.5%) of untreated and 0/14 (0%) of saline-injected fetuses. No hemidefect showed complete coverage in this series.

Comparative Analysis between Defect Coverage and Gene Expression

Table 2 compares paracrine factor expression at the defect and bone marrow as well as bone marrow MSC clonality marker expression in fetuses with covered versus uncovered defects. Defect level analysis was performed in 58 fetuses with determinate defect histology and available defect RT-qPCR data, while bone marrow analysis was performed in 48 fetuses with determinate defect histology and available bone marrow RT-qPCR data. Defect coverage was significantly associated with downregulation of both epidermal growth factor (*Egf*) and fibroblast growth factor-2 (*Fgf-2*) expression at the defect site ($p = 0.031$ and $p = 0.042$, respectively; Fig. 3), though not at the bone marrow.

There was no other significant difference in gene expression between fetuses with covered and uncovered defects. However, there was a trend toward decreased transforming growth factor-beta-1 (*Tgfb-1*) and *CD45* expression in the bone marrow between covered and uncovered defects ($p = 0.065$ and $p = 0.065$, respectively). Therefore, *Tgfb-1* and *CD45* expression was further explored using binary cutoffs established by the maximal Youden index from each variable's ROC curve that best discriminated coverage. For *Tgfb-1*, a fold difference cutoff of 1.55 was established. Covered defects were significantly more likely than uncovered defects to have a *Tgfb-1* fold expression of <1.55 (LRT: $p = 0.021$; OR: 8.1). For *CD45*, a fold difference threshold of 1.32 was established. Covered defects were significantly more likely than uncovered defects to have a *CD45* fold expression of <1.32 (LRT: $p = 0.028$; OR: 5.1) (Fig. 4).

Gene Expression by Treatment Group

Table 3 compares overall paracrine factor expression at the defect site between treatment groups, including re-

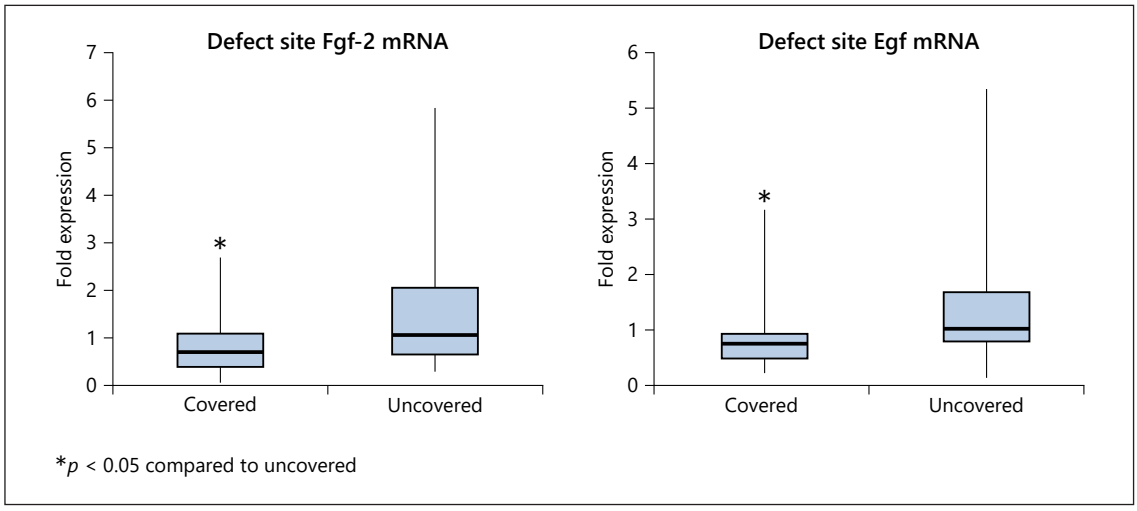

Fig. 3. *Fgf-2* (left) and *Egf* (right) mRNA fold expression at the defect site, respectively, between fetuses with covered and uncovered defects. Data are expressed as median, interquartile range, and full range. Reported *p* values reflect results from Mann-Whitney U test analysis. *Egf*, epidermal growth factor; *Fgf-2*, fibroblast growth factor-2.

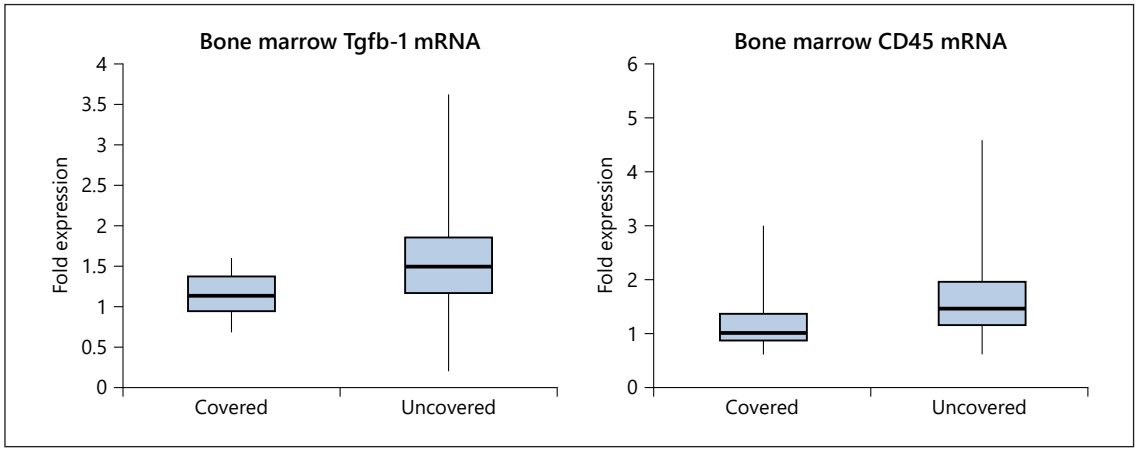

Fig. 4. *Tgfb-1* (left) and *CD45* (right) mRNA fold expression in the fetal bone marrow, respectively, between fetuses with covered and uncovered defects. Data are expressed as median, interquartile range, and full range. *Tgfb-1*, transforming growth factor-beta-1.

sults from both Mann-Whitney U testing (n = 102) and quantile regression analysis controlling for defect area to total dorsum area ratio (n = 95). Similarly, Tables 4 and 5 compare paracrine factor expression and MSC clonality marker expression in the bone marrow between treatment groups including normal fetuses used for reference (afMSC: n = 25; saline: n = 30; untreated: n = 24; normal: n = 32), with comparisons performed by the Mann-Whitney U test only. There were no significant overall differences between the afMSC-injected group and both the untreated and saline-injected groups concurrently in paracrine factor expression at either the defect or the bone marrow, or in bone marrow MSC marker expression. However, there were several significant differences in bone marrow paracrine factor and MSC clonality marker expression between the retinoic acid-exposed fetuses in all 3 groups and normal fetuses.

Correlational Analysis between Defect and Bone Marrow Gene Expression

Spearman's correlation analysis between paracrine factor expression at the defect and bone marrow was performed for 79 fetuses with both defect and bone marrow RT-qPCR data. This demonstrated a significant positive

Table 3. Defect paracrine factor fold expression bytreatment group

Paracrine factor	Group comparison	*p* value (Mann-Whitney U test)	Quantile regression model adjusting for defect area: total dorsum area ratio		
			adjusted difference in medians	95% CI	*p* value
Fgf-2/b-Fgf	afMSC versus saline	0.088	0.58	(0.02, 1.14)	0.043
	afMSC versus untreated	0.151	0.12	(−0.43, 0.66)	0.673
	Saline versus untreated	0.626	−0.46	(−1.04, 0.11)	0.112
Vegf-a	afMSC versus saline	**0.007***	0.74	(0.19, 1.29)	**0.009***
	afMSC versus untreated	0.189	0.23	(−0.30, 0.76)	0.396
	Saline versus untreated	0.093	−0.51	(−1.08, 0.05)	0.073
Egf	afMSC versus saline	0.169	0.44	(−0.15, 1.04)	0.144
	afMSC versus untreated	0.363	0.16	(−0.41, 0.74)	0.574
	Saline versus untreated	0.390	−0.28	(−0.89, 0.33)	0.368
Tgfb-3	afMSC versus saline	0.526	−0.18	(−0.57, 0.21)	0.356
	afMSC versus untreated	0.787	−0.15	(−0.53, 0.22)	0.427
	Saline versus untreated	0.480	0.03	(−0.37, 0.43)	0.880
Tgfb-1	afMSC versus saline	0.192	0.29	(−0.15, 0.74)	0.197
	afMSC versus untreated	0.531	−0.06	(−0.49, 0.37)	0.793
	Saline versus untreated	0.530	−0.35	(−0.81, 0.11)	0.133
Cox-2	afMSC versus saline	0.055	0.84	(0.23, 1.44)	**0.007***
	afMSC versus untreated	0.461	0.14	(−0.44, 0.73)	0.634
	Saline versus untreated	0.305	−0.70	(−1.32, −0.08)	0.028

Vegf-a, vascular endothelial growth factor-a; *Egf*, epidermal growth factor; *Fgf-2*, fibroblast growth factor-2; *Tgfb-3*, transforming growth factor-beta-3; *Tgfb-1*, transforming growth factor-beta-1; afMSC, amniotic fluid-derived mesenchymal stem cell. * Statistically significant based on a Bonferroni-adjusted *p* value threshold of $p < 0.017$.

correlation between transforming growth factor-beta-3 (*Tgfb-3*) expression at the defect and vascular endothelial growth factor-a (*Vegf-a*) expression at the bone marrow ($r = 0.228$, $p = 0.043$) as well as a significant negative correlation between *Tgfb-1* expression at the defect and *Tgfb-3* expression at the bone marrow ($r = -0.247$, $p = 0.028$).

Discussion

Our central hypothesis that the bone marrow is a fundamental component of the host's response to TRASCET was informed not only by our own previous findings, as listed above, but also by the abundant body of work on the role of the bone marrow in various forms of postnatal tissue repair [12–16]. These extensive previous data highlight the role of the bone marrow in this complex process, including: a chaperone effect upon resident cells and their derivatives, changes in marrow cell profile and turnover, and adaptations in select paracrine factor activity. This study is the first mechanistic investigation of TRASCET in the setting of spina bifida. It could not possibly cover all potential processes at play. We decided to focus on those more likely related to reported postnatal data, specifically involving paracrine activity and bone marrow stem cell clonality.

It is widely known that the bone marrow's relevance to tissue repair derives mostly from its core MSC population, which has long been shown to secrete a variety of paracrine factors that promote wound healing, angiogenesis, and immunomodulation [12–16]. Our results show significant downregulation of *Fgf-2* and *Egf* at the defect site in fetuses with covered spina bifida defects when compared with those with no evidence of coverage. Although at first this may seem counterintuitive, we postulate that the association between the downregulation of certain paracrine factors with the presence of neoskin suggests the possibility of a negative feedback loop regulating local paracrine activity once coverage has started or already been achieved. Indeed, downregulation of para-

Table 4. Bone marrow paracrine factor fold expression by treatment group

Paracrine factor	Group comparison	*p* value (Mann-Whitney U test)
Fgf-2/b-Fgf	afMSC versus saline	0.094
	afMSC versus untreated	0.920
	Saline versus untreated	0.169
	afMSC versus normal	**0.004***
	Saline versus normal	0.128
	Untreated versus normal	**0.006***
Vegf-a	afMSC versus saline	0.398
	afMSC versus untreated	0.020
	Saline versus untreated	0.009
	afMSC versus normal	0.040
	Saline versus normal	0.375
	Untreated versus normal	**<0.001***
Tgfb-3	afMSC versus saline	0.612
	afMSC versus untreated	0.459
	Saline versus untreated	0.347
	afMSC versus normal	**<0.001***
	Saline versus normal	**<0.001***
	Untreated versus normal	**<0.001***
Tgfb-1	afMSC versus saline	0.589
	afMSC versus untreated	0.952
	Saline versus untreated	0.715
	afMSC versus normal	0.037
	Saline versus normal	**0.004***
	Untreated versus normal	0.009

Fgf-2, fibroblast growth factor-2; *Vegf-a*, vascular endothelial growth factor-a; *Tgfb-3*, transforming growth factor-beta-3; *Tgfb-1*, transforming growth factor-beta-1; afMSC, amniotic fluid-derived mesenchymal stem cell. * Statistically significant based on a Bonferroni-adjusted *p* value threshold of $p < 0.0083$.

Table 5. Bone marrow MSC clonality analysis by treatment group

Stem cell marker	Group comparison	*p* value (Mann-Whitney U test)
Ptprc/CD45	afMSC versus saline	0.039
	afMSC versus untreated	0.156
	Saline versus untreated	0.159
	afMSC versus normal	0.131
	Saline versus normal	**<0.001***
	Untreated versus normal	**0.001***
Snai1	afMSC versus saline	0.946
	afMSC versus untreated	0.447
	Saline versus untreated	0.486
	afMSC versus normal	**0.001***
	Saline versus normal	**<0.001***
	Untreated versus normal	**<0.001***
Vcam-1/CD106	afMSC versus saline	0.250
	afMSC versus untreated	0.134
	Saline versus untreated	0.009
	afMSC versus normal	**<0.001***
	Saline versus normal	**<0.001***
	Untreated versus normal	**<0.001***
Mcam/CD146	afMSC versus saline	0.589
	afMSC versus untreated	0.093
	Saline versus untreated	0.126
	afMSC versus normal	0.016
	Saline versus normal	0.105
	Untreated versus normal	**0.004***
Msx2	afMSC versus saline	0.728
	afMSC versus untreated	0.386
	Saline versus untreated	0.433
	afMSC versus normal	**<0.001***
	Saline versus normal	**0.001***
	Untreated versus normal	**<0.001***
Thy1/CD90	afMSC versus saline	0.447
	afMSC versus untreated	0.379
	Saline versus untreated	0.175
	afMSC versus normal	**0.002***
	Saline versus normal	**0.007***
	Untreated versus normal	**<0.001***
Endoglin/CD105	afMSC versus saline	0.437
	afMSC versus untreated	0.308
	Saline versus untreated	0.035
	afMSC versus normal	**<0.001***
	Saline versus normal	**<0.001***
	Untreated versus normal	**<0.001***

MSC, mesenchymal stem cell; afMSC, amniotic fluid-derived mesenchymal stem cell. * Statistically significant based on a Bonferroni-adjusted *p* value threshold of $p < 0.0083$.

crine factors in the setting of wound healing has been previously reported. For example, a study using a rodent model of tympanic membrane perforation showed that the expression of certain paracrine factors (keratinocyte growth factor and transforming growth factor-alpha) peaked early on during healing and decreased 7 days thereafter, suggesting a dynamic process involving delayed negative feedback [17]. Another study using a fetal rodent injury model found that *Fgf-2* expression levels were decreased up to 72 h after wound formation, especially in the setting of scarless repair as documented at E16 [18]. Our findings showing an association between downregulation of *Fgf-2* and *Egf* and patent defect coverage are consistent with those of previous literature. While this association does not equate to definitive mechanistic proof, it does provide important mechanistic clues and

will guide further investigation focusing on earlier stages in the repair process.

Within the bone marrow, our results showed a significant association between *Tgfb-1* downregulation and increased defect coverage, mirroring the putative negative feedback on paracrine activity seen at the defect level. We also found a significant association between the presence of coverage and downregulation of *CD45* expression, one of the markers of hematopoietic stem cell (HSC)-derived lineages that is not present in MSCs. It has long been known that bone marrow MSCs constitute a heterogeneous population, with clonal MSCs exhibiting different morphologies, growth rates, cell densities, and gene and protein expression profiles. These different MSC clones are thought to exist in a hierarchical structure. Phenotypic "fingerprints" that predict biological activity of a given MSC clone can be compared by quantitative expression of classical stem cell markers relevant to the cellular behavior. While this initial investigation did not explore the granularity of marrow MSC heterogeneity, our results indicate a shift in the balance between MSC and HSC clones. We found that defect coverage was associated a relative preponderance of MSCs, which further corroborates the role of the bone marrow in the formation of the neoskin.

We also observed significant differences in paracrine factor and MSC clonality marker expressions within the bone marrow in each of the retinoic-acid-exposed treatment groups when compared with the bone marrow from normal fetuses used as the reference tissue. It is possible that these differences may simply reflect direct biological effects of retinoic acid on the bone marrow and bone development, as described in multiple prior studies [19–21]. However, these results may also reflect a shared bone marrow response to the presence of the spina bifida defect in fetuses from all 3 experimental groups.

We must recognize inherent limitations of this study design. In order to correlate histological defect coverage and RT-qPCR data from the same defect, we were required to split each defect into 2 hemidefects. Because of the presence of bone bearing various degrees of deformity in that area, this was technically challenging and was a determining factor in the sizeable proportion of histological preparations being deemed inappropriate for proper coverage assessment. Moreover, the corresponding hemidefects from the same fetus were assumed to have the same degree of coverage, if any, for comparative histological and RT-qPCR analyses, though of course this could not have been histologically proven. Finally, the plethora of previous data on postnatal tissue repair, including bone marrow analyses, demonstrates a variety of complex and interrelated processes at play. It would be beyond the scope of this study, if at all possible, to include all possible contributors to the host's response to TRASCET.

Nevertheless, the present work does support our hypothesis that TRASCET-induced coverage of experimental spina bifida, in variable degrees, with a host-derived neoskin derives from host bone marrow activity, via an apparent magnification of naturally occurring phenomena. Further analyses informed by this insight may lead to enhancements of the TRASCET approach as well as possible additional strategies of nonsurgical induction of prenatal coverage of spina bifida.

Statement of Ethics

This study was approved by the Boston Children's Hospital Institutional Animal Care and Use Committee (IACUC) under protocol # 18-07-3757R. All animal care was in compliance with the Guide for the Care and Use of Laboratory Animals.

Conflict of Interest Statement

The authors have no conflicts to declare.

Funding Sources

This work was supported by the Kevin and Kate McCarey Fund for Surgical Research at Boston Children's Hospital.

Author Contributions

S.P.L.: data collection, data analysis, and manuscript preparation. S.A.T.: data collection. A.V.C.: data collection. I.K.: data collection and manuscript preparation. D.Z.: data analysis. D.O.F.: study design, data analysis, and manuscript preparation.

References

1 Fauza DO. Transamniotic stem cell therapy: a novel strategy for the prenatal management of congenital anomalies. Pediatr Res. 2018;83:241–8.
2 Klein JD, Turner CG, Steigman SA, Ahmed A, Zurakowski D, Eriksson E, et al. Amniotic mesenchymal stem cells enhance normal fetal wound healing. Stem Cells Dev. 2011;20(6):969–76.
3 Dionigi B, Ahmed A, Brazzo J 3rd, Connors JP, Zurakowski D, Fauza DO. Partial or complete coverage of experimental spina bifida by simple intra-amniotic injection of concentrated amniotic mesenchymal stem cells. J Pediatr Surg. 2015;50(1):69–73.

4 Dionigi B, Brazzo JA 3rd, Ahmed A, Feng C, Wu Y, Zurakowski D, et al. Trans-amniotic stem cell therapy (TRASCET) minimizes Chiari-II malformation in experimental spina bifida. J Pediatr Surg. 2015;50(6):1037–41.
5 Feng C, D Graham C, Connors JP, Brazzo J 3rd, Zurakowski D, Fauza DO. A comparison between placental and amniotic mesenchymal stem cells for transamniotic stem cell therapy (TRASCET) in experimental spina bifida. J Pediatr Surg. 2016;51(6):1010–3.
6 Shieh HF, Tracy SA, Hong CR, Chalphin AV, Ahmed A, Rohrer L, et al. Transamniotic stem cell therapy (TRASCET) in a rabbit model of spina bifida. J Pediatr Surg. 2019;54(2):293–6.
7 Shieh HF, Ahmed A, Rohrer L, Zurakowski D, Fauza DO. Donor mesenchymal stem cell kinetics after transamniotic stem cell therapy (TRASCET) for experimental spina bifida. J Pediatr Surg. 2018;53(6):1134–6.
8 Shieh HF, Ahmed A, Tracy SA, Zurakowski D, Fauza DO. Fetal bone marrow homing of donor mesenchymal stem cells after transamniotic stem cell therapy (TRASCET). J Pediatr Surg. 2018 Jan;53(1):174–7.
9 Kaviani A, Perry TE, Dzakovic A, Jennings RW, Ziegler MM, Fauza DO. The amniotic fluid as a source of cells for fetal tissue engineering. J Pediatr Surg. 2001;36(11):1662–5.
10 Klein JD, Fauza DO. Amniotic and placental mesenchymal stem cell isolation and culture. Methods Mol Biol. 2011;698:75–88.
11 Danzer E, Schwarz U, Wehrli S, Radu A, Adzick NS, Flake AW. Retinoic acid induced myelomeningocele in fetal rats: characterization by histopathological analysis and magnetic resonance imaging. Exp Neurol. 2005;194(2):467–75.
12 Dimarino AM, Caplan AI, Bonfield TL. Mesenchymal stem cells in tissue repair. Front Immunol. 2013;4:201.
13 Gerson SL. Mesenchymal stem cells: no longer second class marrow citizens. Nat Med. 1999;5(3):262–4.
14 Hong HS, Lee J, Lee E, Kwon YS, Lee E, Ahn W, et al. A new role of substance P as an injury-inducible messenger for mobilization of CD29(+) stromal-like cells. Nat Med. 2009;15(4):425–35.
15 Minguell JJ, Allers C, Lasala GP. Mesenchymal stem cells and the treatment of conditions and diseases: the less glittering side of a conspicuous stem cell for basic research. Stem Cells Dev. 2013;22(2):193–203.
16 Phinney DG, Prockop DJ. Concise review: mesenchymal stem/multipotent stromal cells: the state of transdifferentiation and modes of tissue repair--current views. Stem Cells. 2007;25(11):2896–902.
17 Ishibashi T, Shinogami M, Ishimoto SI, Yoshida K, Kaga K. Induction of KGF, basic FGF, and TGFalpha mRNA expression during healing of experimental TM perforations. Acta Otolaryngol. 1998;118(5):701–4.
18 Dang CM, Beanes SR, Soo C, Ting K, Benhaim P, Hedrick MH, et al. Decreased expression of fibroblast and keratinocyte growth factor isoforms and receptors during scarless repair. Plast Reconstr Surg. 2003;111(6):1969–79.
19 Feng T, Cong Y, Qin H, Benveniste EN, Elson CO. Generation of mucosal dendritic cells from bone marrow reveals a critical role of retinoic acid. J Immunol. 2010;185(10):5915–25.
20 Hashimoto-Hill S, Friesen L, Park S, Im S, Kaplan MH, Kim CH. RARα supports the development of Langerhans cells and langerin-expressing conventional dendritic cells. Nat Commun. 2018;9(1):3896.
21 Hengesbach LM, Hoag KA. Physiological concentrations of retinoic acid favor myeloid dendritic cell development over granulocyte development in cultures of bone marrow cells from mice. J Nutr. 2004;134(10):2653–9.